Acta Crystallographica Section F
Structural Biology and Crystallization Communications
ISSN 1744-3091

Crystallization and preliminary X-ray diffraction analysis of human dipeptidyl peptidase 10 (DPPY), a component of voltage-gated potassium channels

Gustavo Arruda Bezerra,[a] Elena Dobrovetsky,[b] Alma Seitova,[b] Sirano Dhe-Paganon[b] and Karl Gruber[a]*

[a]Institute of Molecular Biosciences, University of Graz, Humboldtstrasse 50/3, A-8010 Graz, Austria, and [b]Department of Physiology and Structural Genomics Consortium, University of Toronto, MaRS Centre, South Tower, 101 College Street, Suite 700, Toronto, ON M5G 1L7, Canada

Correspondence e-mail: karl.gruber@uni-graz.at

Received 6 October 2011
Accepted 22 December 2011

Dipeptidyl peptidase 10 (DPP10, DPPY) is an inactive peptidase associated with voltage-gated potassium channels, acting as a modulator of their electrophysiological properties, cell-surface expression and subcellular localization. Because potassium channels are important disease targets, biochemical and structural characterization of their interaction partners was sought. DPP10 was cloned and expressed using an insect-cell system and the protein was purified *via* His-tag affinity and size-exclusion chromatography. Crystals obtained by the sitting-drop method were orthorhombic, belonging to space group $P2_12_12_1$ with unit-cell parameters a = 80.91, b = 143.73, c = 176.25 Å. A single solution with two molecules in the asymmetric unit was found using the structure of DPP6 (also called DPPX; PDB entry 1xfd) as the search model in a molecular replacement protocol.

1. Introduction

The voltage-gated potassium channel family (Kv) constitutes the most diverse class of ion channels in the nervous system, not only owing to the presence of 12 subfamilies (Kv1–Kv12) but also owing to the large number of auxiliary proteins that interact with the Kv pore-forming α-subunits (Ren *et al.*, 2005; Herson & Adelman, 2003).

Kv4 channels mediate the subthreshold-operating A-type K^+ current in neurons (I_{SA}). They regulate the firing frequency and synaptic integration/plasticity, which have been implicated in neuronal disorders (Maffie & Rudy, 2008). It is well established that potassium channel-interacting proteins (KChIPs) and the dipeptidyl aminopeptidase-like proteins DPP6 (also called DPPX) and DPP10 (also called DPPY) associate with Kv4 channels, affecting their electrophysiological properties, cell-surface expression and subcellular localization (Marionneau *et al.*, 2011).

DPP6 and DPP10 are DPPIV-related members of the prolyl oligopeptidase family (both sharing approximately 30% sequence identity with DPPIV) and belong to the S9B serine protease subfamily. The representative of the family and the best characterized member, DPPIV (also known as CD26), possesses an enzymatic activity that has been implicated in important physiological processes, and structure-based inhibitors have successfully been commercialized for the treatment of type 2 diabetes (Yazbeck *et al.*, 2009). In DPP6 and DPP10, however, the serine of the catalytic triad is replaced by an aspartic acid or a glycine, respectively (Fig. 1), thereby abolishing peptidase activity.

DPP6 and DPP10 are glycosylated single-pass type II transmembrane proteins that share close to 50% identity to each other and are involved in the modulation of voltage-gated channels belonging to the mammalian Kv4 subfamily (Qi *et al.*, 2003; Kin *et al.*, 2001). While DPP6 is broadly found in human organs, to date DPP10 has only been described in human brain, adrenal gland and pancreas, displaying tissue-selective expression of splicing variants, which suggests that these isoforms may play distinct functional roles (Takimoto *et al.*, 2006). Both proteins accelerate the activation and inactivation of Kv4.3 channel gating with distinct biophysical properties, very likely

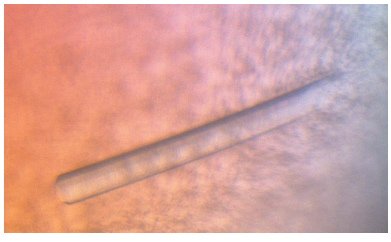

owing to structural differences between the two proteins (Ren *et al.*, 2005). This disparity in modulation is very likely to be central to the correct propagation of neuronal somatodendritic A-type K^+ currents. Moreover, comparable discrepancies in the recovery kinetics from an inactivation state have also been observed in Kv4.2 channels co-expressed with DPP10 and DPP6 in *Xenopus* oocytes and CHO cells (Jerng *et al.*, 2005).

Since DPP6 and DPP10 are components of the neuronal Kv4 channels, these proteins are potential drug targets for diseases such as Parkinson's, schizophrenia and temporal lobe epilepsy (Djurovic *et al.*, 2010; Singh *et al.*, 2006). Indeed, truncated forms of DPP10 are associated with neurodegenerative conditions such as Alzheimers, diffuse Lewy body disease and fronto-temporal dementia (Chen *et al.*, 2008). Additionally, polymorphisms in the gene encoding DPP10 are associated with asthma (Allen *et al.*, 2003). The molecular basis of the association between these DPPs and the channel subunits remains largely unknown. Therefore, we initiated a project aimed at determining the three-dimensional structure of DPP10.

2. Materials and methods

2.1. Cloning and expression

Human dipeptidyl peptidase 10 was cloned from a Mammalian Gene Collection cDNA template (AT23-C8) into the pFHMSP-LIC-N vector using an In-Fusion CF Dry-Down PCR Cloning Kit (Clontech), resulting in a plasmid named dpp10.0058-0796.134F03 (SDC134F03). This plasmid was transformed into *Escherichia coli* DH10Bac cells (Invitrogen) and a mini-prep was performed to obtain recombinant viral DNA bacmid. SF9 cells (Invitrogen) were transfected with the bacmid using Cellfectin reagent (Invitrogen) and recombinant baculovirus was generated. Viral stock was amplified from P1 to P3. Subsequently, Sf9 cells grown in Serum Free Medium (HyClone SFX-Insect) at a density of 3.5 million cells per millilitre of medium and with a viability not less than 97% were infected with 10 ml of P3 viral stock per litre of cell culture. Cell-culture medium was collected after 3–4 d incubation on a shaker at 100 rev min^{-1} and 300 K when cell viability dropped to 45–65%.

2.2. Purification

The culture medium was centrifuged at 14 000*g* for 15 min and the pH of the supernatant was adjusted to 7.5 at 298 K by titrating with 50 m*M* Tris–HCl pH 8.0 and 1.5 *M* NaCl. A 3.2 l volume of medium was mixed with 30 ml pre-equilibrated Ni–NTA Superflow beads (Qiagen) and shaken (Talboys) on ice for 1 h. The resin was transferred to a 100 ml gravity column, washed with 300 ml washing buffer (50 m*M* Tris–HCl pH 8.0, 500 m*M* NaCl, 5 m*M* imidazole) and the protein was eluted with 30–40 ml elution buffer [50 m*M* Tris–HCl pH 8.0, 500 m*M* NaCl, 300 m*M* imidazole, 5%(*v*/*v*) glycerol]. In order to increase the protein yield, the culture medium from the first round was mixed with a new 30 ml batch of pre-equilibrated Ni–NTA Superflow beads (Qiagen) and treated as described above. The eluted protein was further purified by size-exclusion chromatography (SEC) on a HiLoad 16/60 Superdex 75 (GE Healthcare) column equilibrated with 50 m*M* Tris–HCl pH 8.0, 100 m*M* NaCl. The chromatogram from the gel-filtration column showed one major protein peak that consisted of DPP10, as confirmed by SDS–PAGE analysis.

The N-terminal His tag was removed by incubation with TEV protease at a TEV:DPP10 ratio of 1:50. The reaction was incubated at 277 K for 2 d. Cleavage was confirmed by SDS–PAGE analysis and the TEV protease as well as the cleaved His tag were removed by passing the sample through a 1 ml HisTrap FF crude column (GE Healthcare) which had been equilibrated with the buffer used for SEC (see above).

Purified protein was concentrated to a final value of 2 mg ml^{-1} using 15 ml concentrators with an appropriate molecular-weight cutoff (Amicon Ultra-15 10 000 MWCO, Millipore). The average yield was 0.8 mg purified protein per litre of cell-culture medium. Coomassie-stained SDS–PAGE showed that the product was pure and LC/MS mass spectrometry (Agilent 1100 Series) showed that the purified protein had a molecular mass that was slightly (3 Da) less than the expected 83 662.6 Da.

2.3. Crystallization

Crystallization trials were performed at the Structural Genomics Consortium (SGC) high-throughput platform in Toronto using the sitting-drop vapour-diffusion method in a 96-well Intelli-Plate (Art Robbins Instruments) at 293 K by mixing equal volumes (0.5 µl) of 2 mg ml^{-1} protein solution and reservoir solution using a Mosquito robot (TTP LabTech).

Crystallization trials were initially set up using the in-house screens Red Wing and SGC-I. Each screen consists of 96 conditions that were chosen from commercial and published screens with an emphasis on conditions with the highest known success rates. The detailed formulations of these screens can be found on the SGC website (http://www.sgc.utoronto.ca/SGC-WebPages/toronto-technology-crystallization.php). Crystals formed within 2–4 weeks over 100 µl reservoir consisting of 20%(*w*/*v*) PEG 1500 (Sigma–Aldrich), 0.2 *M* $MgCl_2$, 0.1 *M* sodium cacodylate pH 5.5. Most DPP10 crystals were of rectangular shape, with average dimensions of about 0.1 × 0.05 × 0.005 mm (as judged from comparison with the 0.1 mm cryoloop used for crystal mounting). Rod-like crystals such as that shown in Fig. 2 with approximate dimensions of 0.2 × 0.01 × 0.01 mm were the exception.

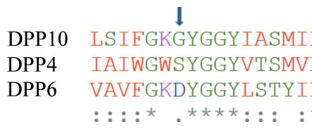

Figure 1
Sequence alignment of DPP10, DPP4 and DPP6 showing the region around the consensus sequence (G*X*S*X*G). The arrow emphasises the substitution of the catalytic serine in DPP4 by glycine in DPP10 and by aspartic acid in DPP6. The alignment was generated with *ClustalW* (Larkin *et al.*, 2007; Goujon *et al.*, 2010). The colouring scheme distinguishes hydrophobic (red), polar (green), negatively charged (blue) and positively charged (magenta) residues. Asterisks indicate identical residues, whereas colons denote highly similar residues and periods denote less similar residues with respect to physicochemical properties.

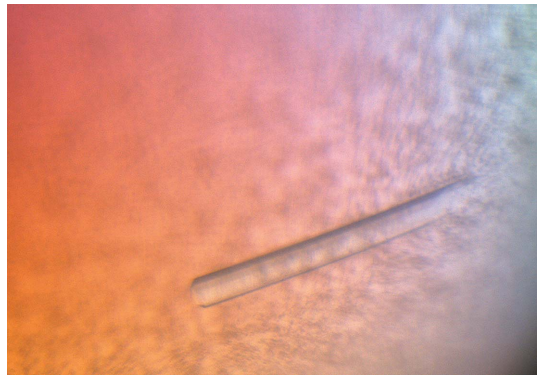

Figure 2
Crystal of DPP10 with approximate dimensions of 0.2 × 0.01 × 0.01 mm grown using the sitting-drop vapour-diffusion method at 293 K.

Crystals were flash-cooled in liquid nitrogen after being cryoprotected by passage through a solution of 25%(*w*/*v*) PEG 1500, 0.2 *M* $MgCl_2$, 0.1 *M* sodium cacodylate pH 5.5, 10%(*v*/*v*) glycerol. Optimization of the crystallization conditions was attempted but did not improve the diffraction of the resulting crystals.

2.4. Structure determination

Diffraction data were collected on beamline 19-ID at the Advanced Photon Source (APS), Chicago, USA. The data were processed using *MOSFLM* (Leslie, 2006; Battye *et al.*, 2011) and *SCALA* (Evans, 2006). Details of data collection and processing are summarized in Table 1. The structure was solved by molecular replacement using *BALBES* (Long *et al.*, 2008). The molecular-replacement model is currently being refined using *PHENIX* (Adams *et al.*, 2010) and *Coot* (Emsley & Cowtan, 2004).

3. Results and discussion

DPP10 and DPP6 consist of an intracellular N-terminal domain followed by a transmembrane helix and an extracellular 'catalytic' domain (Ren *et al.*, 2005). A large number of nested loop constructs were tested, only one of which, comprised of the extracellular residues 57–797, crystallized. Attempts to optimize the initial conditions did not improve the diffraction pattern of the crystals. For data collection, 180 images were recorded to a maximum resolution of 2.4 Å (the limit of the detector) at 100 K. However, based on $R_{\rm merge}$ and signal-to-noise ratios [$I/\sigma(I)$], data above 3.5 Å resolution were excluded (Fig. 3). Data processing with *MOSFLM* (Leslie, 2006; Battye *et al.*, 2011) yielded a primitive orthorhombic lattice with space group $P2_12_12_1$, which was also confirmed by *POINTLESS* (Evans, 2006).

According to the calculated Matthews coefficient (Matthews, 1968), the asymmetric unit could be comprised of two or three molecules, corresponding to approximate solvent contents of 60 and 40%, respectively. The *BALBES* molecular-replacement pipeline (Long *et al.*, 2008) produced a clear solution employing the structure of DPP6 (PDB entry 1xfd; Strop *et al.*, 2004) as a search template with two molecules in the asymmetric unit. The initial R and $R_{\rm free}$ values were 0.454 and 0.444, respectively, and improved to 0.269 and 0.367 after preliminary refinement within *BALBES*. The presence of two molecules in the asymmetric unit is in agreement with biochemical data showing that the protein occurs as a dimer (Ren *et al.*, 2005). Oligomerization of DPP10 and DPP6 is very likely to play a fundamental role in the modulation of voltage-gated potassium channels (Strop *et al.*, 2004). DPP6 and DPP10 have also been speculated to form heterodimers with each other because of their pronounced sequence identity.

Structure refinement is under way, after which a detailed analysis of the dimer interface in DPP10 and comparison of its structure with that of DPP6 will allow a better understanding of the specificity of (hetero)-dimer formation and will help to establish the molecular details involved in the modulation of the neuronal Kv4 channels.

Table 1
Data-collection statistics for DPP10.

Values in parentheses are for the outer resolution shell.

Beamline	APS 19-ID
Wavelength (Å)	0.97943
Unit-cell parameters (Å)	a = 80.91, b = 143.73, c = 176.25
Space group	$P2_12_12_1$
Resolution range (Å)	66.55–3.50 (3.69–3.50)
Completeness (%)	99.8 (99.3)
Multiplicity	4.8 (4.6)
$R_{\rm merge}$†	0.217 (0.666)
$\langle I/\sigma(I)\rangle$	6.9 (2.6)
Total reflections	126610 (17456)
Unique reflections	26229 (3767)

† $R_{\rm merge} = \sum_{hkl}\sum_i |I_i(hkl) - \langle I(hkl)\rangle| / \sum_{hkl}\sum_i I_i(hkl)$.

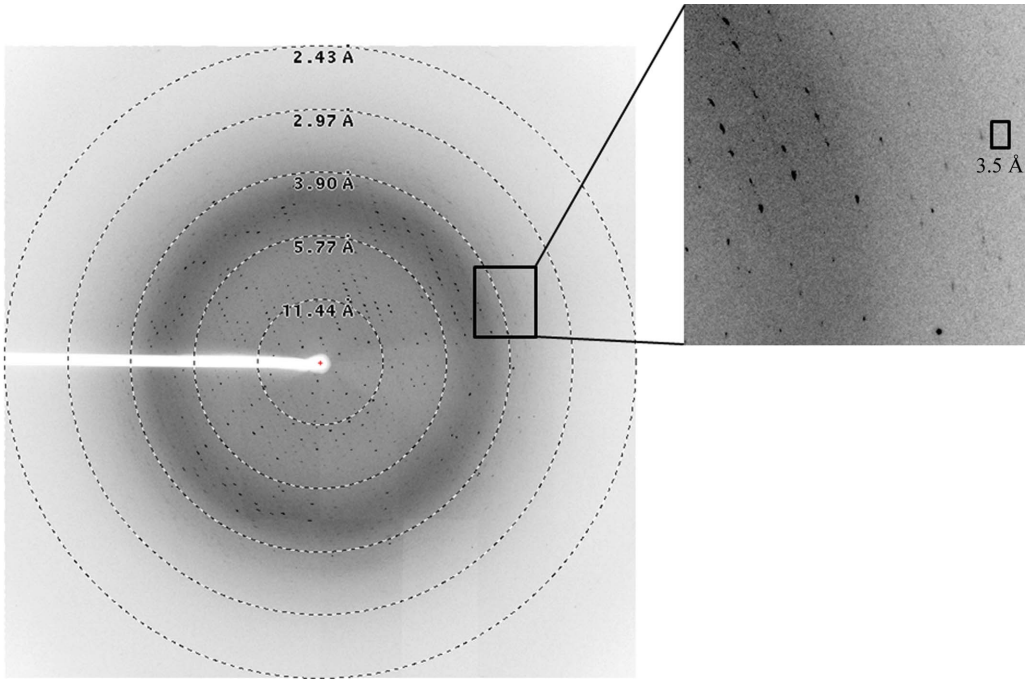

Figure 3
Diffraction pattern of DPP10. The inset shows the high-resolution limit of the data set. The figure was generated using the program *ADXV* (http://www.scripps.edu/~arvai/adxv.html).

We thank Lissete Crombet (SGC Toronto) for cloning services and the beamline staff at APS for support during diffraction data collection. Funding was provided by the Austrian Science Funds (FWF) through project W901 (Doktoratskolleg 'Molecular Enzymology'), the Canadian Institutes for Health Research, the Canadian Foundation for Innovation, Genome Canada through the Ontario Genomics Institute, GlaxoSmithKline, Karolinska Institutet, the Knut and Alice Wallenberg Foundation, the Ontario Innovation Trust, the Ontario Ministry for Research and Innovation, Merck & Co. Inc., the Novartis Research Foundation, the Swedish Agency for Innovation Systems, the Swedish Foundation for Strategic Research and the Wellcome Trust.

References

Adams, P. D. *et al.* (2010). *Acta Cryst.* D**66**, 213–221.
Allen, M. *et al.* (2003). *Nature Genet.* **35**, 258–263.
Battye, T. G. G., Kontogiannis, L., Johnson, O., Powell, H. R. & Leslie, A. G. W. (2011). *Acta Cryst.* D**67**, 271–281.
Chen, T., Shen, X.-F., Chegini, F., Gai, W.-P. & Abbott, C. A. (2008). *Clin. Chem. Lab. Med.* **46**, A13.
Djurovic, S., Gustafsson, O., Mattingsdal, M., Athanasiu, L., Bjella, T., Tesli, M., Agartz, I., Lorentzen, S., Melle, I., Morken, G. & Andreassen, O. A. (2010). *J. Affect. Disord.* **126**, 312–316.
Emsley, P. & Cowtan, K. (2004). *Acta Cryst.* D**60**, 2126–2132.
Evans, P. (2006). *Acta Cryst.* D**62**, 72–82.
Goujon, M., McWilliam, H., Li, W., Valentin, F., Squizzato, S., Paern, J. & Lopez, R. (2010). *Nucleic Acids Res.* **38**, W695–W699.
Herson, P. S. & Adelman, J. P. (2003). *Neuron*, **37**, 370–372.
Jerng, H. H., Kunjilwar, K. & Pfaffinger, P. J. (2005). *J. Physiol.* **568**, 767–788.
Kin, Y., Misumi, Y. & Ikehara, Y. (2001). *J. Biochem.* **129**, 289–295.
Larkin, M. A., Blackshields, G., Brown, N. P., Chenna, R., McGettigan, P. A., McWilliam, H., Valentin, F., Wallace, I. M., Wilm, A., Lopez, R., Thompson, J. D., Gibson, T. J. & Higgins, D. G. (2007). *Bioinformatics*, **23**, 2947–2948.
Leslie, A. G. W. (2006). *Acta Cryst.* D**62**, 48–57.
Long, F., Vagin, A. A., Young, P. & Murshudov, G. N. (2008). *Acta Cryst.* D**64**, 125–132.
Maffie, J. & Rudy, B. (2008). *J. Physiol.* **586**, 5609–5623.
Marionneau, C., Townsend, R. R. & Nerbonne, J. M. (2011). *Semin. Cell Dev. Biol.* **22**, 145–152.
Matthews, B. W. (1968). *J. Mol. Biol.* **33**, 491–497.
Qi, S. Y., Riviere, P. J., Trojnar, J., Junien, J.-L. & Akinsanya, K. O. (2003). *Biochem. J.* **373**, 179–189.
Ren, X., Hayashi, Y., Yoshimura, N. & Takimoto, K. (2005). *Mol. Cell. Neurosci.* **29**, 320–332.
Singh, B., Ogiwara, I., Kaneda, M., Tokonami, N., Mazaki, E., Baba, K., Matsuda, K., Inoue, Y. & Yamakawa, K. (2006). *Neurobiol. Dis.* **24**, 245–253.
Strop, P., Bankovich, A. J., Hansen, K. C., Garcia, K. C. & Brunger, A. T. (2004). *J. Mol. Biol.* **343**, 1055–1065.
Takimoto, K., Hayashi, Y., Ren, X. & Yoshimura, N. (2006). *Biochem. Biophys. Res. Commun.* **348**, 1094–1100.
Yazbeck, R., Howarth, G. S. & Abbott, C. A. (2009). *Trends Pharmacol. Sci.* **30**, 600–607.